Effect of iron doping on the magnetic structure of $TbBaCo_2O_{5.5}$ layered perovskite

2008 J. Phys.: Condens. Matter 20 335228

(http://iopscience.iop.org/0953-8984/20/33/335228)

J. Phys.: Condens. Matter **20** (2008) 335228 (6pp) doi:10.1088/0953-8984/20/33/335228

Effect of iron doping on the magnetic structure of $TbBaCo_2O_{5.5}$ layered perovskite

I O Troyanchuk[1], D V Karpinsky[1,3] and F Yokaichiya[2]

[1] Scientific-Practical Materials Research Centre NAS of Belarus, P. Brovka str. 19, 220072 Minsk, Belarus
[2] Hahn-Meitner Institute, Glienicker str. 100, D-14109 Berlin, Germany

E-mail: karpinsky@ifttp.bas-net.by

Received 8 April 2008, in final form 15 July 2008
Published 31 July 2008
Online at stacks.iop.org/JPhysCM/20/335228

Abstract

The crystal and magnetic structures of $TbBaCo_{1.9}Fe_{0.1}O_{5.43}$ have been studied by neutron diffraction and magnetization measurements. It is shown that spontaneous magnetization develops at $T_N = 305$ K and decreases abruptly below 200 K. The crystal structure is described in the space group *Pmmm*, on a $2a_p^*a_p^*2a_p$ unit cell. It was shown that the extra oxygen vacancies are located mainly in the pyramidal sublattice, thus making tetrahedra. Magnetic structure in the high-temperature magnetic phase consists of ferromagnetic and G-type antiferromagnetic components, while in the low-temperature phase only the G-type component exists with a $2a_p^*2a_p^*2a_p$ magnetic unit cell. The ferromagnetic component results from canting magnetic moments of Co^{3+} ions which were found to be predominantly in the high-spin state in pyramids. The refined values of the magnetic moments of the Co^{3+} ions in the octahedra indicate a mixed high–low-spin state. It is assumed that non-collinear magnetic structure results from a concurrence between positive and negative exchange interactions as well as magnetocrystalline anisotropy in the pyramidal sublattice. Using the concept of non-collinear magnetic structure, the giant anisotropic magnetoresistive effect in layered cobaltites is explained.

(Some figures in this article are in colour only in the electronic version)

1. Introduction

The layered perovskites $LnBaCo_2O_{5.5}$ (Ln = lanthanide) have attracted much attention due to the interplay between magnetic and magnetotransport properties [1–4]. The crystal structure of these compounds has an alternating linkage of Ba^{2+} and Ln^{3+} layers along the *c*-axis and layers of CoO_5 pyramids and CoO_6 octahedra along the *a*- or *b*-axes [3].

As a result of ordering of Ln^{3+} and Ba^{2+} ions as well as of oxygen vacancies, the crystal structure is described with unit cell $a_p^*2a_p^*2a_p$ in the space group *Pmmm*. The $LnBaCo_2O_{5.5}$ compounds exhibit the following transitions: antiferromagnet–'ferromagnet' in the temperature range 200 K $\leqslant T <$ 260 K, 'ferromagnet'–paramagnet (250 K $< T <$ 300 K) and metal–insulator (300 K $< T <$ 370 K) depending on Ln ion size [1–3]. According to the neutron diffraction studies the 'ferromagnetic' phase consists of G-type antiferromagnetic ($2a_p^*2a_p^*2a_p$) and ferromagnetic components, while the low-temperature antiferromagnetic phase has magnetic unit cell of $2a_p^*2a_p^*4a_p$ type [5–8]. The transition antiferromagnet–'ferromagnet' leads to a drop of the resistivity and a giant magnetoresistance effect [1–4]. The reason for the interplay between magnetic and magnetotransport properties is not yet clear. In order to understand magnetotransport properties, a detailed description of the magnetic structure in both phases is necessary. Several studies of the magnetic structure of $LnBaCo_2O_{5.5}$ compounds have been performed with diverging results [5–12]. According to [8, 12] the magnetic structure is non-collinear in both antiferromagnetic and ferromagnetic phases. The Co^{3+} ions in octahedra adopt

[3] Author to whom any correspondence should be addressed.

the low-spin state [8, 12], whereas in pyramids they are in the intermediate-spin state. In works [5, 6] it was suggested that the correct space group is *Pmma* and the crystal structure is described with a $2a_p^*2a_p^*2a_p$ supercell. In this model Co^{3+} ions in both pyramidal and octahedral sublattices are located in non-equivalent sites and magnetic structure can be described by a collinear model for both 'ferromagnetic' and antiferromagnetic phases. However, a neutron diffraction study of a $TbBaCo_2O_{5.5}$ single crystal has not revealed any additional peaks associated with a $2a_p^*2a_p^*2a_p$ crystal structure supercell [12]. Furthermore the 'ferromagnetic' phase was found in fast cooled $TbBaCo_2O_{5.46}$ with a simple crystal structure supercell $a_p^*a_p^*2a_p$ [10]. This compound remains 'ferromagnetic' at all temperatures below $T_N = 240$ K [10]. So, further studies are necessary to establish an appropriate model of the magnetic structure.

Very intricate properties have been revealed in $TbBaCo_2O_{5.5-x/2}$ doped with Fe^{3+} ions [4, 13]. In $TbBaCo_{2-x}Fe_xO_{5.5-x/2}$ below $x = 0.1$ orthorhombic distortion slightly increases with increasing Fe^{3+} content and suddenly disappears above $x = 0.1$. The temperature of the 'ferromagnet'–paramagnet transition increases while the temperature of the 'ferromagnet'–antiferromagnet transition decreases with increasing Fe^{3+} content up to $x = 0.1$. Transition into the tetragonal phase ($x > 0.10$) leads to a collapse of the ferromagnetic phase. The jump of conductivity as well as thermal hysteresis associated with the 'ferromagnet'–antiferromagnet transition becomes larger with Fe doping within the orthorhombic phase. The antiferromagnetic phase becomes proof against an external magnetic field. A Mössbauer study has revealed that Fe^{3+} ions predominantly occupy two strongly distorted positions [13]. It should be noted that such behavior is in strong contrast to the physical properties of $YBaCo_2O_{5.44}$ with a similar oxygen content deviation from the ideal stoichiometric value of 5.5 [6].

In order to understand the magnetic and transport properties of layered cobaltite doped with Fe^{3+} ions we have undertaken a neutron diffraction study of $TbBaCo_{1.9}Fe_{0.1}O_{5+\gamma}$ composition. We have established that the low-temperature antiferromagnetic phase is of G-type with a simple $2a_p^*2a_p^*2a_p$ magnetic unit cell, in contrast to a $2a_p^*2a_p^*4a_p$ unit cell for undoped samples. Our data strongly support the model of the non-collinear magnetic structure for the description of magnetic and magnetotransport properties of $LnBaCo_2O_{5.5}$ type compounds.

2. Experimental details

A sample of $TbBaCo_{1.9}Fe_{0.1}O_{5+\gamma}$ nominal composition has been prepared from Tb_4O_7, $BaCO_3$, CoO and Fe_2O_3 taken in a stoichiometric ratio. Synthesis was performed at $T = 1150\,^\circ$C in air followed by the sample cooling down to room temperature at a rate of $50\,^\circ$C h^{-1}. The magnetization was measured with a MPMS-5 magnetometer. The neutron diffraction data were collected using the FIREPOD high-resolution powder diffractometer (E9) at the Hahn-Meitner Institute, Berlin. The wavelength was 1.791 Å. Powder patterns were recorded at 315, 215, and 130 K. Data analysis was performed by the Rietveld method using the FullProf program package [14].

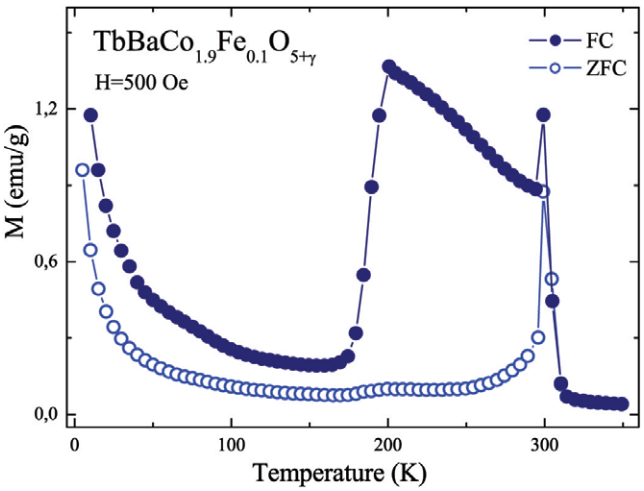

Figure 1. The temperature dependences of the magnetization for $TbBaCo_{1.9}Fe_{0.1}O_{5+\gamma}$ measured in the FC and ZFC modes at $H = 500$ Oe.

3. Results and discussion

The results of measurements of zero field cooled (ZFC) and field cooled (FC) magnetization in a field of 500 Oe on warming are shown in figure 1. Both ZFC and FC magnetizations exhibit a sharp maxima at $T = 300$ K which indicates the transition into a paramagnetic state. In the temperature interval 20–170 K the FC magnetization decreases strongly with lowering temperature. In this temperature range ZFC magnetization changes very little, thus indicating a huge magnetic anisotropy. It should be noted that ZFC and FC magnetizations do not coincide below 170 K down to liquid helium temperature due to the presence of a small spontaneous magnetization.

Analysis of the neutron diffraction pattern at 315 K has shown that the sample consists of a major perovskite-like phase and a small amount of second phase. The good agreement between calculated and observed profiles of neutron powder diffraction (NPD) patterns was reached using the *Pmmm* space group with a $2a_p^*a_p^*2a_p$ unit cell for the major phase. The refinement in the *Pmma* space group with $2a_p^*2a_p^*2a_p$ unit cell leads to the same factors of reliability as the refinement in terms of the *Pmmm* model.

The additional reflections near $2\theta = 100.4$ and 135.5° on the 315 K pattern clearly testify to the presence of the second phase. These additional peaks do not resolve at low temperatures as orthorhombic distortions of the major phase become smaller. The content of the second phase is small so it is difficult to determine the space group unambiguously. The $TbBaCo_{1.9}Fe_{0.1}O_{5+\gamma}$ compound is about the concentration transition from orthorhombic to tetragonal phase [13, 15]. It was shown [13, 15] that in the concentration range $0.1 \leqslant x \leqslant 0.14$ both orthorhombic and tetragonal phases may coexist. The tetragonal samples ($P4/mmm$ space group) do not exhibit spontaneous magnetization above the helium temperature [13], whereas fast cooled $TbBaCo_2O_{5.43}$ (*Pmmm* space group; $a_p^*a_p^*2a_p$ metric) shows spontaneous magnetization without an antiferromagnet–'ferromagnet' transition [10]. One can

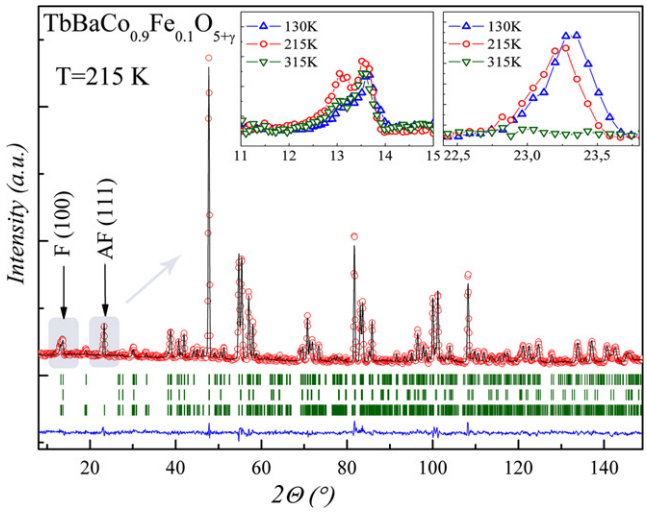

Figure 2. Refinement pattern for $TbBaCo_{1.9}Fe_{0.1}O_{5+\gamma}$ at 215 K obtained from neutron powder diffraction data. The arrows denote the major magnetic contribution. Temperature variations of the (100) and (111) peak are shown in the insets. The two upper vertical dashes denote Bragg reflection positions for crystallographic phases (*Pmmm* space group with a $2a_p^* a_p^* 2a_p$ unit cell for the major phase and $P4/mmm$ space group with a $a_p^* a_p^* 2a_p$ unit cell for the second phase). The lower one indicates the magnetic phase.

suggest that the presence of spontaneous magnetization below the antiferromagnet–'ferromagnet' transition (figure 1) is associated with the second phase. It was found that using the $P4/mmm$ or *Pmmm* space group with $a_p^* a_p^* 2a_p$ metric gave a good description of the second phase. However, taking into account the results of magnetic measurements (figure 1) the description of the second phase in the *Pmmm* $a_p^* a_p^* 2a_p$ model is the more preferred interpretation. The data analysis has shown the ratio of these phases to be about 9:1. The second phase parameters at 315 K are $a = 3.890$ Å, $b = 3.886$ Å, $c = 7.535$ Å in the *Pmmm* space group and $a = 3.887$ Å, $b = 3.887$ Å, $c = 7.535$ Å in the $P4/mmm$ one.

The observed and calculated profiles of the patterns at $T = 215$ K are presented in figure 2. The results of the refinement of structural parameters are presented in table 1. The value of orthorhombic distortions slightly decreases with decreasing temperature. This is associated with an anisotropic thermal behavior of *a* and *b* unit cell parameters.

One can see from table 1 that the ordering of Ba^{2+} and Tb^{3+} ions is practically complete. The cations and oxygen ions content corresponds to the chemical formula $TbBaCo_{1.9}Fe_{0.1}O_{5.43}$ which denotes the formation of the extra oxygen vacancies. The main part of the extra oxygen vacancies is located within the pyramidal sublattice on the O4 positions, thus making CoO_4 tetrahedra. The remaining part of the oxygen vacancies results in the appearance of pyramids in the octahedral sublattice. The CoO_6 octahedra as well as the CoO_5 pyramids are strongly distorted. These distortions have been interpreted as an indication of the orbital ordering [16, 17].

Analysis of the powder patterns collected at the temperature 215 K shows that there is a set of additional magnetic reflections which could be indexed using a $2a_p^* 2a_p^* 2a_p$ magnetic unit cell (figure 2). Furthermore,

Table 1. The results of crystal and magnetic structure refinements of the NPD data.

Atom	Parameter	130 K	215 K	315 K
	a (Å)	7.7977(1)	7.8165(2)	7.8299(2)
	b (Å)	3.8663(2)	3.8629(1)	3.8643(1)
	c (Å)	7.5162(1)	7.5232(2)	7.5352(2)
	Volume	**226.60**	**227.16**	**227.99**
Tb(1)/Ba(1):	(Wyck.)		(2l)	
	X	0.2676	0.2698	0.2710
	Y	0.5	0.5	0.5
	Z	0.5	0.5	0.5
	Biso (Å^2)	1.0	1.0	1.0
	occ.	100/0	99/1	100/0
Ba(2)/Tb(2):			(2k)	
	X	0.2480	0.2498	0.2473
	Y	0.5	0.5	0.5
	Z	0	0	0
	Biso (Å^2)	0.8	0.8	0.9
		92/8	93/7	92/8
Co(1)/Fe(1):			(2s)	
	X	0.5	0.5	0.5
	Y	0	0	0
	Z	0.2553	0.2548	0.2516
	Biso (Å^2)	1.0	1.1	1.3
Co(2)/Fe(2):			(2q)	
	X	0	0	0
	Y	0	0	0
	Z	0.2544	0.2560	0.2586
	Biso (Å^2)	1.9	1.0	0.7
O(1):			(1a)	
	X	0	0	0
	Y	0	0	0
	Z	0	0	0
	Biso (Å^2)	0.9	0.5	1.6
	occ.	1.0	1.0	1.0
O(2):			(1b)	
	X	0.5	0.5	0.5
	Y	0	0	0
	Z	0	0	0
	Biso (Å^2)	0.6	0.8	1.0
	occ.	0.96	0.96	0.95
O(3):			(1d)	
	X	0.5	0.5	0.5
	Y	0	0	0
	Z	0.5	0.5	0.5
	Biso (Å^2)	1.7	2.2	1.8
	occ.	0.93	0.95	0.94
O(4):			(2r)	
	X	0	0	0
	Y	0.5	0.5	0.5
	Z	0.3137	0.3135	0.3134
	Biso (Å^2)	0.7	0.9	1.5
	occ.	0.98	0.97	0.98
O(5):			(2t)	
	X	0.5	0.5	0.5
	Y	0.5	0.5	0.5
	Z	0.2714	0.2725	0.2739
	Biso (Å^2)	1.6	1.3	1.0
	occ.	1.0	0.99	0.99
O(6):			(4w)	
	X	0.2399	0.2422	0.2422
	Y	0	0	0

Table 1. (Continued.)

Atom	Parameter	130 K	215 K	315 K
	Z	0.2987	0.2960	0.2960
	Biso (Å^2)	0.9	1.2	1.5
	occ.	1.0	1.0	1.0
$Co_{oct}(1)$–O(2) (Å)		1.9190	1.9172	1.8957
$Co_{oct}(1)$–O(3) (Å)		1.8390	1.8444	1.8719
$Co_{oct}(1)$–O(5) (Å)	×2	1.9369	1.9360	1.9395
$Co_{oct}(1)$–O(6) (Å)	×2	2.0530	2.0389	2.0590
$Co_{pent}(2)$–O(1) (Å)		1.9124	1.9259	1.9487
$Co_{pent}(2)$–O(4) (Å)	×2	1.9842	1.9794	1.9758
$Co_{pent}(2)$–O(6) (Å)	×2	1.9013	1.9170	1.9035
Co(2)–O(4)–Co(2)		154.03	154.73	155.86
Co(1)–O(5)–Co(1)		172.84	172.13	170.04
Co(1)–O(6)–Co(2)		161.80	162.20	162.28
R_p (%)/R_{wp} (%)		**5.11/6.48**	**4.52/5.73**	**5.04/6.83**
R_{Bragg} (%)		**9.4**		**8.5**
χ^2		**2.15**	**2.04**	**2.05**
Magnetic moment Co(Fe), μ_B:				
G-type:		pent	pent	
		μ_a=±2.6 μ_B	μ_a=±1.9 μ_B	
		oct	oct	
		μ_a=±0.9 μ_B	μ_a=±0.9 μ_B	—
F-type			$\mu_b = 1.0\ \mu_B$	—
Magnetic R-factor		18.7	17.3/27.3	—

the additional contribution into (100) reflection has been clearly observed. This contribution disappears at 130 K (figure 2, inset). The contribution into reflection (100) corresponds to the ferromagnetic component whereas the appearance of (111), (311), (113), (331), and (313) reflections corresponds to the G-type antiferromagnetic component. The contribution to the G-type antiferromagnetic component increases with decreasing temperature down to 130 K, whereas the ferromagnetic contribution disappears (figure 2). Such behavior of the antiferromagnetic component was observed first for the $LnBaCo_2O_{5.5}$ layered perovskite exhibiting antiferromagnet–'ferromagnet' transition. The low-temperature antiferromagnetic phase of the undoped with iron compounds is described with a more complex $2a_p^*2a_p^*4a_p$ magnetic unit cell [5–10]. The refinement of the magnetic structure at 215 K gives the following values of magnetic moments for the G-type antiferromagnetic component: 1.9 μ_B per Co ion for the pyramidal sublattice and 0.9 μ_B for the octahedral one. The ferromagnetic component is 1.0 μ_B per formula unit directed along the b-axis, whereas the antiferromagnetic component is along the a-axis. All the magnetic moments are placed within the (a, b) plane. Decreasing the temperature down to 130 K leads to increasing magnetic moment up to 2.6 μ_B for the pyramidal sublattice while for the octahedral one it practically does not change.

Both octahedra and pyramids are strongly distorted as was mentioned above. According to [16, 17] the distortion is associated with orbital ordering. For the realization of the orbital ordering the Co^{3+} ions should be in the intermediate-spin state and an ionic component of the chemical bond should be dominant. However, photoemission studies [18] have revealed that the d-electrons of the Co^{3+} in $LnBaCo_2O_{5.5}$ compounds are not localized even in the insulating phase. The refined value of the magnetic moment (see table 1) indicates that the Co^{3+} ions are not in the intermediate-spin state. Furthermore, the distortions of oxygen polyhedra may arise from a mismatch of ionic radii for different ions forming the crystal structure of $LnBaCo_2O_{5.5}$ compounds.

Deviation of oxygen content from the stoichiometric value of 5.5 should lead to the appearance of the Co^{2+} ions instead of the Co^{3+} ones. Structural refinement indicates that oxygen vacancies are concentrated in the O4 positions which link two nearest pyramids along the b-axis (see the table 1). According to a Mössbauer study, the Fe^{3+} ions in $TbBaCo_{1-x}Fe_xO_{5.5-x/2}$ ($x = 0.08$) occupy two strongly distorted non-equivalent positions [13]. We think the Fe^{3+} ions are incorporated in pyramids and tetrahedra within the nominal CoO_5 sublattice. According to resistivity measurements, the jump of conductivity associated with the antiferromagnet–'ferromagnet' transition slightly increases with Fe^{3+} doping [4]. As electrical transport in these compounds is connected mainly with the octahedral sublattice, we suppose that the Co^{2+} ions also accumulate mainly within the pyramidal sublattice, so the octahedral one remains much more regular.

The magnetic moment value in the pyramidal sublattice is 2.6 μ_B per ion at 130 K. This value is significantly more than the 2 μ_B associated with the intermediate-spin state. It was found that magnetic moments of the high-spin Co^{3+} ions in $Sr_2Co_2O_5$ and $BiCoO_3$ are 3.3 and 3.4 μ_B respectively [19, 20]. However, the magnetic moment of the Co^{3+} ion in the high-spin state ($S = 2$) should be about 4 μ_B. So, the present data can hardly be adjusted with a pure ionic model for the Co ions' magnetic moments. In works [21, 22] the Co^{3+} ions in $LaCoO_3$ have been shown to have first excited state corresponding to the high-spin one. Probably this is valid for $LnBaCo_2O_{5.5}$ type compounds. Hence the description of the magnetic state of Co^{3+} ions in $TbBaCo_2O_{5+\gamma}$ doped with iron could be done in terms of a mixed low–high-spin magnetic state. In addition it should be noted that according to the photoemission study [18] e_g and t_{2g} electrons of Co^{3+} ions are delocalized even in the insulating phase of $LnBaCo_2O_{5.5}$ compounds, therefore an itinerant magnetism approach is more appropriate for a description of the magnetic state. The results of an NMR study of $EuBaCo_2O_{5.5}$ are in agreement with a mixed low–high-spin state model [23].

The magnetic moments in both sublattices seem to be very sensitive to the method of preparation, presence of oxygen vacancies, or impurities. For example, according to [8] in a $TbBaCo_2O_{5.5}$ single crystal a magnetic moment per Co^{3+} ion is 1.5 μ_B for pyramids and about zero for octahedra. The strong increase of magnetic moment value under Fe doping observed in the present work seems to result from the increasing ionic component of the chemical bond due to both substitution of Co^{3+} with Fe^{3+} and extra oxygen vacancies located at the pyramidal sublattice.

Both 'ferromagnetic' and antiferromagnetic phases in $TbBaCo_{1.9}Fe_{0.1}O_{5.43}$ have the G-type magnetic structure with

a $2a_p^* 2a_p^* 2a_p$ magnetic unit cell. In this magnetic structure there are only two different magnetic positions for both CoO_5 and CoO_6 layers. The transition into the antiferromagnetic phase leads to a substantial increase of magnetic moments in the pyramidal sublattice, whereas magnetic moments in the octahedra remain practically the same. These results can be easily understood in the non-collinear model of the magnetic structure of the 'ferromagnetic' phase.

Apparently in the ferromagnetic phase the angle between magnetic moments of the Co^{3+} ions in the pyramidal sublattice in the direction of the a-axis is about 30°. In the antiferromagnetic phase the magnetic structure seems to be collinear and aligned along the b-axis because the $2a_p^* 2a_p^* 2a_p$ magnetic unit cell is preserved. Remember that in the undoped $TbBaCo_2O_{5.5}$ the low-temperature antiferromagnetic phase remains non-collinear and the magnetic unit cell contains four sites for magnetic ions which leads to a $2a_p^* 2a_p^* 4a_p$ magnetic supercell [12].

In order to understand the origin of the non-collinear magnetic structure it is necessary to consider exchange interactions in the pyramidal sublattice. We suppose exchange interactions in the pyramidal sublattice to be negative in the case when nearest pyramids have a common oxygen ion and positive if not. In this case all the interactions within the (a, b) plane are negative whereas along the c-axis negative and positive ones are alternated. This leads to a frustration of magnetic interactions and the non-collinear magnetic structure in the some temperature range could be more favorable than the simple collinear one. The spin–orbital interaction seems also to be a very important factor leading to canting of the magnetic moments. Really the measurements of magnetic and magnetotransport properties performed on a single crystal have revealed a huge magnetocrystalline anisotropy as well as giant anisotropic magnetoresistance [24]. A number of non-collinear magnetic structures in different magnetic materials have been understood in terms of the itinerant magnetism approach with relativistic interactions [25]. Doping with Fe^{3+} stabilizes the collinear antiferromagnetic structure at low temperatures because all the interactions Fe^{3+}–Fe^{3+}, Fe^{3+}–Co^{2+}, Fe^{3+}–Co^{3+} seem to be strongly antiferromagnetic. At high Fe doping ($x > 0.1$) the orthorhombic symmetry transforms to tetragonal symmetry, leading to the ferromagnetic component disappearing [4, 13]. The ferromagnetic component collapse is caused by the random distribution of the octahedra and pyramids in the tetragonal phase.

In works [5, 6] the non-collinear solution has been overruled on the basis of symmetry analysis. However, the non-collinear magnetic structures in $LnBaCo_2O_{5.5}$ compounds seem to be a result of a subtle balance between positive and negative exchange interactions and magnetocrystalline anisotropy. So the symmetry consideration should be more complex, as it was given in [5, 6].

Using the concept of non-collinear magnetism, one can try to explain the peculiarities of magnetic and transport properties of the Fe-doped layered cobaltites, associated with the 'ferromagnet'–antiferromagnet transition: large thermal hysteresis, enhanced jump of conductivity, and proof against external magnetic field [4, 13]. The antiferromagnetic phase in Fe-doped cobaltites is collinear whereas in undoped compounds the antiferromagnetic phase remains non-collinear [12]. One can suggest that non-collinear antiferromagnetic and ferromagnetic phases have ground states very close in energy, so a relatively small external field induces a metamagnetic transition. In contrast to Fe-doped cobaltites, the energy gap between collinear antiferromagnetic and non-collinear antiferromagnetic phases is much larger, thus leading to proof against an external field and large thermal hysteresis. According to [26], the transition into the non-collinear phase leads to strong changes in the vicinity of the Fermi level so the strong jump of conductivity is expected. Really in the non-collinear model the antiferromagnetic component is aligned along the a-axis whereas along the b-axis the pure ferromagnetic component is realized, thus leading to a jump of conductivity at the antiferromagnet–'ferromagnet' transition.

It should be noted that there is another series of layered oxides with chemical formula close to $Sr_{0.75}Y_{0.25}CoO_{2.625}$ [27]. The structure of these oxides contains layers of CoO_6 octahedra alternating with partially disordered CoO_4 and CoO_5 layers. It was been found that these compounds exhibit relatively small spontaneous magnetization (0.2 μ_B per Co^{3+}) below $T_N = 335$ K [28]. Note that both T_N and spontaneous magnetization values are very close to those for $TbBaCo_2O_{5.5}$ doped with iron. Similar to the $LnBaCo_2O_{5.5}$ series, the $Sr_{0.77}Y_{0.23}CoO_{2.63}$ compound exhibits increasing magnetization with temperature increase. Our preliminary neutron diffraction data show that this compound is characterized by simple G-type magnetic structure down to 2 K. One can suppose that the origin of spontaneous magnetization for both $LnBaCo_2O_{5.5}$ and $Sr_{0.75}Ln_{0.25}CoO_{2.625}$ is similar. In both series of compounds the non-collinear magnetic structure may arise due to the competition between ferromagnetic and antiferromagnetic interactions within oxygen deficient layers.

Summarizing the results, we have found that the magnetic lattice of the Fe-doped $LnBaCo_2O_{5+\delta}$ compounds in both antiferromagnetic and 'ferromagnetic' phases can be described with a simple G-type magnetic cell in a $2a_p^* 2a_p^* 2a_p$ metric. In the early works [5–12] the magnetic lattice of the antiferromagnetic phase has been described using a more complex superstructure with the $2a_p^* 2a_p^* 4a_p$ metric. In the latter case the *Pmma* space group is used [5, 6] and four magnetic sites can be distinguished both in pyramidal and octahedral sublattices, so the magnetic lattice can be described in the collinear model [5, 6]. The G-type magnetic structure is characterized by two magnetic sites in both sublattices. Taking into account that the low-temperature antiferromagnetic phase has a pure G-type structure the magnetic structure of the 'ferromagnetic' phase can only be described in terms of a non-collinear arrangement of magnetic moments.

Acknowledgments

We are grateful to Yu P Chernenkov for the fruitful discussion. The work was supported partly by the Fund for Fundamental Research of Belarus (Project F08R-081) and by the European Commission under the 6th Framework Program through the

Key Action: Strengthening the European Research Area, Research Infrastructures, contract no. RII3-CT-2003-505925 (NMI3).

References

[1] Martin C, Maignan A, Pelloquin D, Nguyen N and Raveau B 1997 *Appl. Phys. Lett.* **71** 1421

[2] Troyanchuk I O, Kasper N V, Khalyavin D D, Szymczak H, Szymczak R and Baran M 1998 *Phys. Rev. Lett.* **80** 3380

[3] Maignan A, Martin C, Pelloquin D, Nguyen N and Raveau B 1999 *J. Solid State Chem.* **142** 247

[4] Troyanchuk I O, Chobot A N, Khalyavin D D, Szymczak R and Szymczak H 2006 *JETP* **95** 748

[5] Plakhty V P, Chernenkov Yu P, Barilo S N, Podlesnyak A, Pomjakushina E, Moskvin E V and Gavrilov S V 2005 *Phys. Rev.* B **71** 214407

[6] Khalyavin D D, Argyriou D N, Amann U, Yaremchenko A A and Kharton V V 2007 *Phys. Rev.* B **75** 134407

[7] Fauth F, Suart E, Caignaert V and Mirebeau I 2002 *Phys. Rev.* B **66** 184421

[8] Soda M, Yuasui Y, Fujita T, Miyashita T, Sata M and Kakura K 2003 *J. Phys. Soc. Japan* **72** 1729

[9] Taskin A A, Lavrov A N and Ando Y 2003 *Phys. Rev. Lett.* **90** 227201

[10] Khalyavin D D, Troyanchuk I O, Kasper N V, Huang Q, Lynn J W and Szymczak H 2002 *J. Mater. Res.* **17** 838

[11] Soda M, Yuasui Y, Ito M, Iikubo S, Sata M and Kakura K 2004 *J. Phys. Soc. Japan* **73** 2857

[12] Soda M, Yasui Y, Kobayashi Y, Fujita T, Sato M and Kakurai K 2006 *J. Phys. Soc. Japan* **75** 104708

[13] Kopcewicz M, Khalyavin D D, Troyanchuk I O, Szymczak H, Szymczak R, Logvinovich D J and Naumovich E N 2003 *J. Appl. Phys.* **93** 479

[14] Rodrıguez-Carvajal J 1993 *Physica* B **55** 192

[15] Khalyavin D D, Balagurov A M, Beskrovnyi A I, Troyanchuk I O, Sazonov A P, Tsipis E V and Kharton V V 2004 *J. Solid State Chem.* **177** 2068

[16] Moritomo Y, Akimoto T, Takeo M, Machida A, Nishibori E, Takata M, Sakata M, Ohoyama K and Nakamura A 2000 *Phys. Rev.* B **61** R13325

[17] Pomjakushina E, Conder K and Pomjakushin V 2006 *Phys. Rev.* B **73** 113105

[18] Takubo K, Son J-Y, Mizokawa T, Soda M and Sato M 2006 *Phys. Rev.* B **73** 075102

[19] Belik A *et al* 2006 *Chem. Mater.* **18** 798

[20] Rodriguez J, Gonzalez-Calbet J M and Grenier J C 1987 *Solid State Commun.* **62** 231

[21] Haverkort M W, Hu Z and Cezar J C 2006 *Phys. Rev. Lett.* **97** 176405

[22] Podlesnyak A *et al* 2006 *Phys. Rev. Lett.* **97** 247208

[23] Kubo H, Zenmyo K, Itoh M, Nakayama N, Mizota T and Ueda Y 2004 *J. Magn. Magn. Mater.* **272–276** 581

[24] Taskin A A, Lavrov A N and Ando Y 2003 *Phys. Rev. Lett.* **90** 227201

[25] Sandratskii L M 1998 *Adv. Phys.* **47** 91

[26] Lizárraga R, Nordström L, Bergqvist L, Bergman A, Sjöstedt E, Mohn P and Eriksson O 2004 *Phys. Rev. Lett.* **93** 107205

[27] Istomin S Ya, Grims J, Svensson G, Drozhzhin O A, Kozhevnikov V L, Antipov E V and Attfield J P 2003 *Chem. Mater.* **15** 4012

[28] Kobayashi W, Ishiwata S, Terasaki I, Takano M, Grigoraviciute I, Yamauchi H and Karppinen M 2005 *Phys. Rev.* B **72** 104408